Supporting Information

Structure of Small Yttrium Monoxide Clusters, Chemical Bonding, and Photoionization: Threshold Photoionization and Density Functional Theory Investigations

Varun Vinayak Deshpande, [a,b] Vaibhav Chauhan,[a] Debashis Bandyopadhyay,[c] Anakuthil Anoop,[d] and Soumen Bhattacharyya[*a,b]

[a]Atomic & Molecular Physics Division, Bhabha Atomic Research Centre, Mumbai 400 085, India.
[b]Homi Bhabha National Institute, Anushaktinagar, Mumbai 400 094, India.
[c]Physics Department, Birla Institute of Technology and Science, Pilani 333031, Rajasthan, India.
[d]School of Digital Sciences, Kerala University of Digital Science, Innovation, and Technology, Digital University Kerala, Technopark Phase IV, Pallipuram, Thiruvananthapuram,Kerala – 695317
* Corresponding author's Email: sbhatt@barc.gov.in

This Supporting Information contains the following:

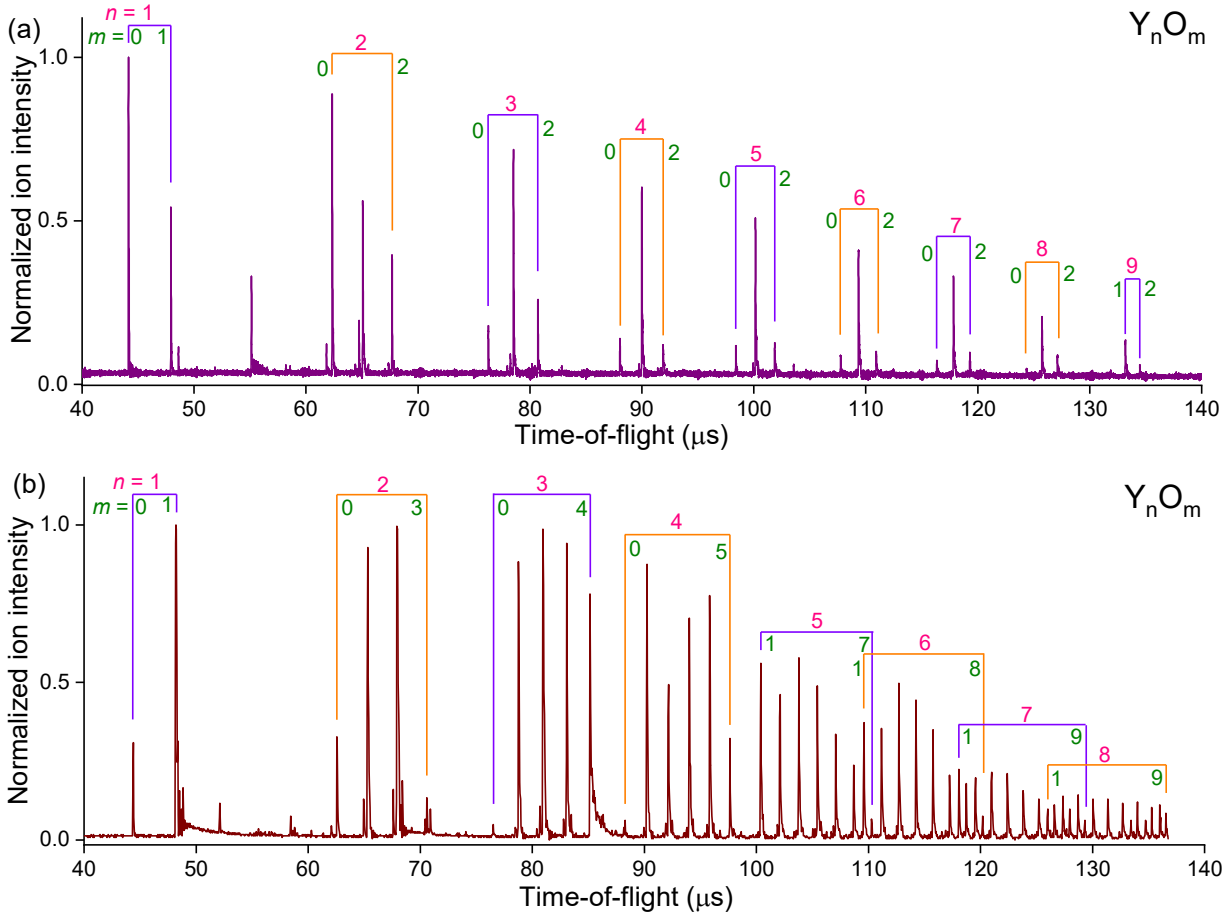

Fig. S1. Mass spectrum of the neutral Y_nO_m clusters (a) with unseeded oxygen, and (b) with 1% oxygen seeding in helium gas.

Table S1. Cartesian coordinates (x, y, z) of the ground state structures of the Y_nO (n = 1–8) clusters.

Neutral				Cation			
YO							
							
Atom	x	y	z	Atom	x	y	z
Y	0.0355911764	0.0002935317	-2.3417444650	Y	0.0213397950	0.0009846174	-2.3237853634
O	-1.0994780016	0.0165581364	-0.9120719108	O	-1.0852215232	0.0156953247	-0.9300311415
Y_2O							
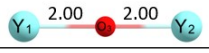				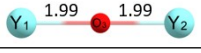			
Y	-0.001060000	0.001110000	2.003359999	Y	-1.986169999	-0.000180000	0.000000000
Y	0.001060000	-0.001570000	-2.003359999	Y	1.986169999	-0.000250000	0.000000000
O	0.000000000	0.002230000	0.000000000	O	0.000000000	0.002080000	0.000000000
Y_3O							
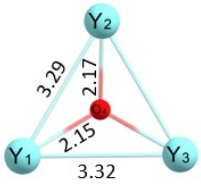				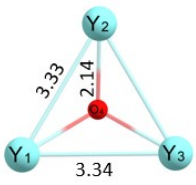			
Y	1.839838411	0.512469781	-0.057100905	y	1.859374366	0.505910530	-0.045098814
Y	-1.346941193	1.344702363	-0.069143439	Y	-1.360921842	1.358824248	-0.049091372
Y	-0.507887166	-1.839599866	-0.054814725	Y	-0.501198259	-1.859230265	-0.042765742
O	0.016207017	-0.013834818	0.941704908	O	0.003962805	-0.001767053	0.897601767

Y_4O

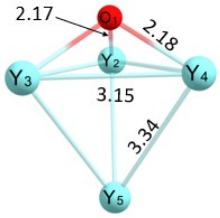

Y	-1.074717650	-1.596245960	0.000000000
Y	1.090087960	0.069266730	-1.573995530
Y	1.090087960	0.069266730	1.573995530
Y	-1.329066050	1.751914210	0.000000000
O	1.090087960	-1.434233270	0.000000000

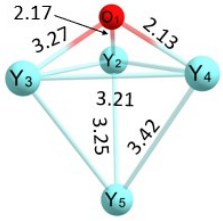

Y	1.426657466	0.081843332	1.606401137
Y	-1.190626103	1.678663333	-0.081721457
Y	-1.190309339	-1.678887154	0.081640572
Y	1.426627641	-0.081601683	-1.606557557
O	-2.300614835	-0.000222327	-0.000206275

Y_5O

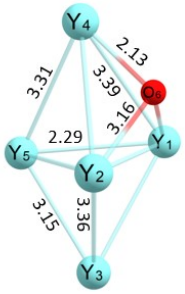

Y	0.011170230	0.944830960	1.681114220
Y	0.011525870	0.943822150	-1.681407240
Y	-2.743789760	0.008975140	-0.000389770
Y	2.678309020	-0.291748760	-0.000117040
Y	-0.225785830	-1.880787410	0.000782970
O	1.309281070	1.340176110	0.000082150

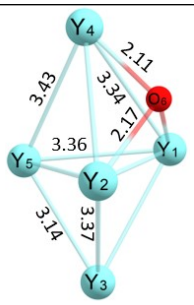

Y	0.035059774	0.932379252	1.682529901
Y	0.035338401	0.931568020	-1.682882399
Y	-2.734530199	0.016022024	-0.000275872
Y	2.671473304	-0.240350813	0.000151666
Y	-0.292794807	-1.961104244	0.000725749
O	1.326164128	1.386753950	-0.000183756

Y_6O

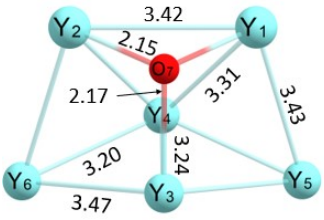

y	0.116436040	1.823983550	1.671753370
Y	0.116436040	1.823983550	-1.671753370
Y	-1.713061630	-0.491924900	0.000000000
Y	1.499362490	-0.675914310	0.000000000
Y	0.116436040	-1.406027690	2.779048790
Y	0.116436040	-1.406027690	-2.779048790
O	-1.228719390	1.618146450	0.000000000

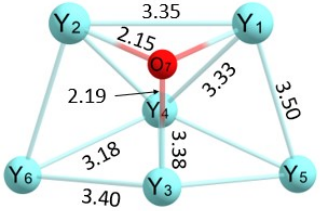

Y	0.088932515	1.829045982	1.675697305
y	0.088939606	1.829051398	-1.675691499
Y	-1.741366369	-0.412786295	-0.000000260
Y	1.634778201	-0.593001975	-0.000004887
Y	0.100133996	-1.542320570	2.620594060
Y	0.100131322	-1.542327797	-2.620593499
O	-1.248223641	1.718558217	-0.000001219

Y_7O

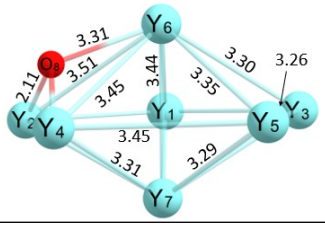

Y	0.732421400	2.847996490	0.028372610
Y	2.913699680	0.228229690	0.097192230
Y	-2.443655220	1.562859670	-0.005549160

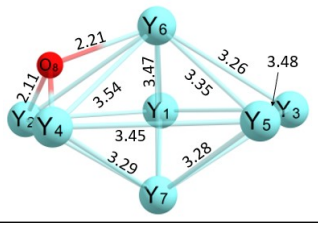

Y	0.653552742	2.898221881	0.051156498
Y	2.922260993	0.162999379	0.091830182
Y	-2.366248657	1.565314269	-0.009888607

Y	0.922895110	-2.759852360	0.107173940	Y	0.987549568	-2.764775992	0.160237896
Y	-2.363018320	-1.695027600	0.076803060	Y	-2.416442935	-1.712925498	0.097733952
Y	-0.084816380	-0.010887490	-1.710429280	Y	-0.062542684	0.050165118	-1.736595229
Y	-0.025881770	0.056116670	1.605741490	Y	-0.035155518	0.050788128	1.567017185
O	1.698233060	-1.118496000	-0.971611330	O	1.666904051	-1.138848215	-0.993798317
Y_8O							
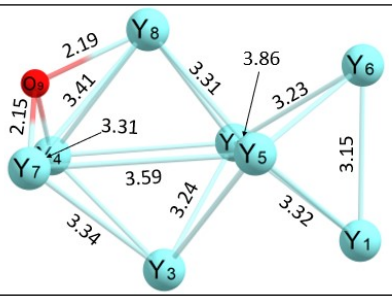				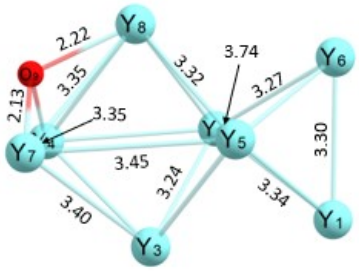			
Y	-2.979839650	-1.547115220	-0.001013890	Y	-1.369055391	-2.594251815	1.600070129
Y	-0.822161980	0.085636840	1.932687040	Y	-1.294902226	-2.428079749	-1.698410286
Y	0.544092410	-2.124319450	-0.001717830	Y	0.253288781	0.480443354	2.339356058
Y	2.746531430	-0.232246280	1.652566880	Y	0.526681234	1.021644051	-2.053125254
Y	-0.822027360	0.088330300	-1.932343100	Y	1.338132755	-1.466940187	-0.012516619
Y	-2.924332580	1.598554440	0.001042970	Y	-1.974057807	0.281448881	-0.000523753
Y	2.746097150	-0.228883310	-1.653097100	Y	2.767468435	1.654723770	0.377233714
Y	0.921374690	2.127283540	0.001610700	Y	-0.199924634	3.219190321	0.364545005
O	2.877546220	1.134700870	0.001288660	O	1.428881375	2.698817105	-0.916628994

Table S2. Vibrational frequencies of neutral and cation clusters of Y_nO (n=1-8). [a] δ_s: symmetric bend; π: out-of-plane bend; ν_s: symmetric stretch; ν_a: asymmetric stretch.

Mode[a]	Symmetry	ω (cm^{-1})	Symmetry	ω (cm^{-1})
	Y_2O		Y_2O^+	
ν_1 (δ_s)	a	92.443	a	41.365
ν_2 (π)	a	92.460	a	41.446
ν_3 (ν_s)	a	265.547	a	271.652
ν_4 (ν_a)	a	838.257	a	703.145
	Y_3O		Y_3O^+	
ν_1	a	138.402	a	129.128
ν_2	a	147.520	a	141.037
ν_3	a	162.098	a	164.284
ν_4	a	336.773	a	381.859
ν_5	a	386.867	a	399.657
ν_6	a	457.737	a	441.234
	Y_4O		Y_4O^+	
ν_1	a	70.09	a	30.43
ν_2	a	73.07	a	60.59
ν_3	a	140.62	a	129.85
ν_4	a	143.88	a	148.67
ν_5	a	149.14	a	151.28
ν_6	a	201.43	a	195.16
ν_7	a	317.73	a	366.12
ν_8	a	349.11	a	379.05
ν_9	a	488.24	a	511.24
	Y_5O		Y_5O^+	
ν_1	a	62.33	a	77.23
ν_2	a	73.62	a	82.54
ν_3	a	95.41	a	97.08
ν_4	a	100.12	a	104.47
ν_5	a	116.73	a	115.95
ν_6	a	131.50	a	128.09

ν_7	a	139.90	a	143.96
ν_8	a	143.46	a	157.13
ν_9	a	169.81	a	169.80
ν_{10}	a	362.92	a	361.50
ν_{11}	a	369.33	a	368.01
ν_{12}	a	443.55	a	454.10
		Y_6O		Y_6O^+
ν_1	a	40.96	a	28.79
ν_2	a	67.74	a	63.18
ν_3	a	78.96	a	87.32
ν_4	a	96.654	a	92.40
ν_5	a	98.061	a	101.49
ν_6	a	110.284	a	105.81
ν_7	a	121.353	a	109.24
ν_8	a	123.588	a	111.82
ν_9	a	127.135	a	136.23
ν_{10}	a	154.105	a	146.90
ν_{11}	a	160.215	a	156.37
ν_{12}	a	179.936	a	181.43
ν_{13}	a	371.265	a	386.77
ν_{14}	a	422.849	a	422.70
ν_{15}	a	426.435	a	423.97
		Y_7O		Y_7O^+
ν_1	a	44.32	a	58.32
ν_2	a	56.65	a	72.60
ν_3	a	64.73	a	73.36
ν_4	a	74.85	a	85.09
ν_5	a	90.74	a	91.96
ν_6	a	92.22	a	99.77
ν_7	a	105.23	a	102.63
ν_8	a	108.94	a	114.78
ν_9	a	118.98	a	123.77
ν_{10}	a	129.84	a	133.94
ν_{11}	a	133.29	a	135.52
ν_{12}	a	147.43	a	146.00
ν_{13}	a	161.23	a	157.76
ν_{14}	a	166.98	a	174.33
ν_{15}	a	202.85	a	201.59
ν_{16}	a	405.45	a	381.79
ν_{17}	a	484.45	a	453.54
ν_{18}	a	498.10	a	501.48
		Y_8O		Y_8O^+
ν_1	a	51.77	a	52.43
ν_2	a	52.81	a	60.62
ν_3	a	62.44	a	64.91
ν_4	a	73.12	a	71.42
ν_5	a	74.13	a	76.32
ν_6	a	94.87	a	94.02
ν_7	a	99.75	a	99.15
ν_8	a	102.51	a	102.18
ν_9	a	105.45	a	107.88
ν_{10}	a	118.63	a	118.39
ν_{11}	a	121.73	a	122.87
ν_{12}	a	124.53	a	129.85
ν_{13}	a	130.02	a	131.23
ν_{14}	a	140.08	a	137.51
ν_{15}	a	143.58	a	143.51
ν_{16}	a	148.47	a	153.66
ν_{17}	a	169.19	a	165.61
ν_{18}	a	201.64	a	202.90
ν_{19}	a	340.56	a	355.86
ν_{20}	a	391.12	a	402.50
ν_{21}	a	472.22	a	478.06

Table S3. Natural Bond Order (NBO) populations and partial charges on atoms on the ground state structures of the neutral Y_nO (n = 3–8) clusters. The atom numbering in the table corresponds to the numbering in Table S1. Population on each atom in the s, p, d atomic orbitals, total population, and partial electronic charge (±q) on an atom are provided.

Atom	s	p	d	Total	q	s	p	d	Total	q
			Neutral Cluster					Cation Cluster		
			Y_3O					Y_3O^+		
Y 1	3.21	6.01	1.07	10.30	0.70	2.88	6.01	1.12	10.01	+0.98
Y 2	3.21	6.01	1.07	10.30	0.70	2.88	6.01	1.12	10.01	+0.98
Y 3	3.65	6.12	1.31	11.08	-0.07	3.10	6.09	1.47	10.66	+0.33
O 3	3.91	5.42	0.00	9.32	-1.33	3.91	5.40	0.00	9.31	-1.31
			Y_4O					Y_4O^+		
Y 1	3.14	6.02	1.37	10.53	+0.47	2.96	6.02	1.33	10.31	+0.68
Y 2	3.14	6.02	1.34	10.50	+0.50	2.96	6.02	1.31	10.29	+0.71
Y 3	3.14	6.02	1.37	10.53	+0.47	2.96	6.02	1.33	10.31	+0.68
Y 4	3.63	6.08	1.34	11.05	-0.05	3.20	6.09	1.39	10.68	+0.32
O 5	3.89	5.50	0.00	9.39	-1.39	3.89	5.50	0.00	9.39	-1.39
			Y_5O					Y_5O^+		
Y 1	3.37	6.05	1.43	10.85	+0.15	3.18	6.04	1.44	10.66	+0.33
Y 2	3.08	6.02	2.09	11.20	-0.20	3.00	6.04	1.95	10.99	+0.01
Y 3	2.98	6.02	1.58	10.58	+0.42	2.85	6.02	1.55	10.42	+0.58
Y 4	2.98	6.02	1.58	10.58	+0.42	2.85	6.02	1.55	10.42	+0.58
Y 5	3.16	6.01	1.22	10.40	+0.60	2.91	6.00	1.19	10.11	+0.89
O 6	3.88	5.51	0.00	9.39	-1.39	3.88	5.51	0.00	9.39	-1.39
			Y_6O					Y_6O^+		
Y 1	2.85	6.04	1.60	10.48	+0.51	2.77	6.04	1.43	10.24	+0.76
Y 2	2.85	6.04	1.61	10.51	+0.49	2.74	6.03	1.60	10.38	+0.62
Y 3	2.85	6.04	1.61	10.51	+0.49	2.74	6.03	1.60	10.38	+0.62
Y 4	3.07	6.05	1.92	11.04	-0.04	2.99	6.05	1.81	10.86	+0.14
Y 5	3.07	6.05	1.92	11.04	-0.04	2.99	6.05	1.81	10.86	+0.14
Y 6	3.06	6.05	1.93	11.04	-0.04	2.93	6.04	1.92	10.90	+0.10
O 7	3.87	5.50	0.00	9.38	-1.38	3.87	5.51	0.00	9.38	-1.38
			Y_7O					Y_7O^+		
Y 1	3.06	6.00	1.20	10.26	+0.74	2.90	6.00	1.21	10.11	+0.89
Y 2	3.06	6.00	1.20	10.26	+0.74	2.90	6.00	1.21	10.11	+0.89
Y 3	3.13	6.01	1.71	10.85	+0.15	3.05	6.01	1.61	10.67	+0.33
Y 4	3.13	6.01	1.71	10.85	+0.15	3.05	6.01	1.61	10.67	+0.33
Y 5	3.00	6.02	1.71	10.74	+0.25	2.95	6.03	1.61	10.59	+0.40
Y 6	2.92	6.00	2.85	11.11	-0.77	2.83	6.01	2.89	11.73	-0.73
Y 7	2.83	6.02	2.01	10.86	+1.40	2.70	6.03	1.98	10.71	+0.29
O 8	3.87	5.52	0.00	9.39	-1.39	3.87	5.52	0.00	9.39	-1.39
			Y_8O					Y_8O^+		
Y 1	3.17	6.03	1.49	10.69	+0.31	3.06	6.03	1.47	10.56	+0.44
Y 2	3.13	6.03	1.55	10.72	+0.28	3.04	6.04	1.50	10.58	+0.41
Y 3	2.94	6.00	2.29	11.24	-0.24	2.90	6.01	2.38	11.29	-0.29
Y 4	2.83	6.00	1.63	10.47	+0.52	2.78	6.00	1.64	10.42	+0.58
Y 5	2.97	6.01	2.53	11.51	-0.51	2.91	6.01	2.37	11.29	-0.29
Y 6	2.97	6.01	2.54	11.52	-0.52	2.90	6.01	2.41	11.32	-0.33
Y 7	2.97	6.01	1.24	10.22	+0.78	2.86	6.01	1.18	10.05	+0.95
Y 8	2.97	6.01	1.24	10.22	+0.78	2.85	6.01	1.20	10.07	+0.93
O 9	3.87	5.53	0.00	9.40	-1.40	3.87	5.53	0.00	9.40	-1.40

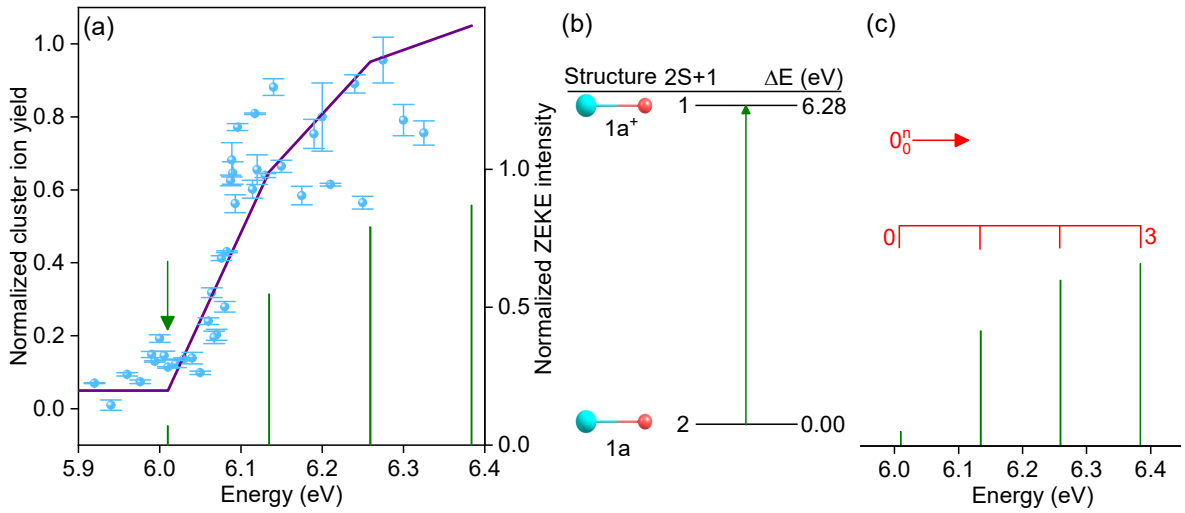

Fig. S2. (a) The simulated PI spectrum of YO (violet solid line) is overlayed against the experimental spectrum (blue spheres). The calculated ZEKE spectrum for the 2→1 ionization process of 1a is shown below the PI spectrum in green. The AIE is labelled with a solid green arrow. (b) DFT calculated the lowest-energy geometric structures and energy levels of the neutral and cation clusters of YO. (c) Simulated ZEKE spectrum for the YO 2→1 ionization transition. Prominent vibronic transitions are assigned in the graph.

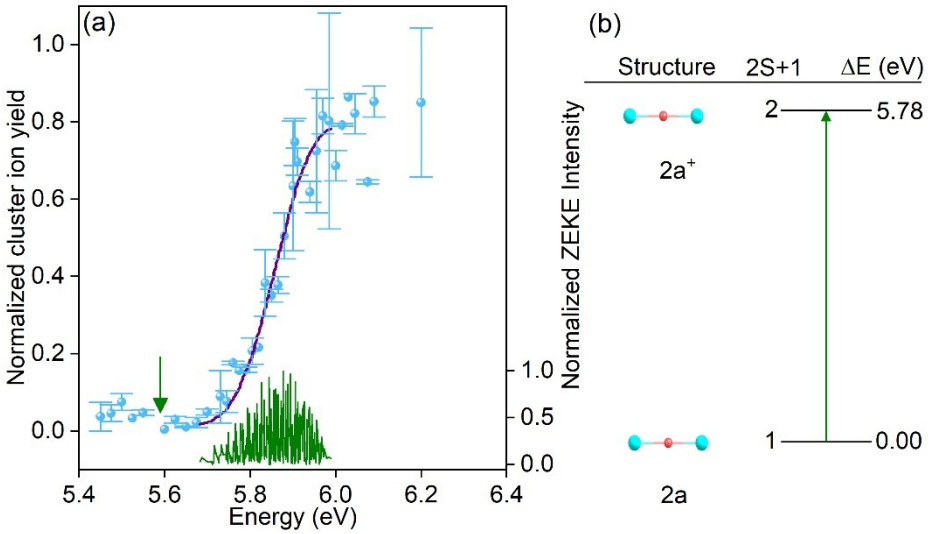

Fig. S3. (a) The simulated PI spectra of Y_2O (violet and red solid lines) is overlayed against the experimental spectrum (blue spheres). The calculated ZEKE spectrum for the 1→2 ionization process for the 2a isomer is shown below the PI spectrum in green. The AIE is labelled with a solid green arrow. (b) DFT calculated the lowest-energy geometric structures and energy levels of the neutral and cation clusters of Y_2O. The peaks in the ZEKE spectrum is dominated by combination bands originating from the two lowest vibrational modes of the neutral.

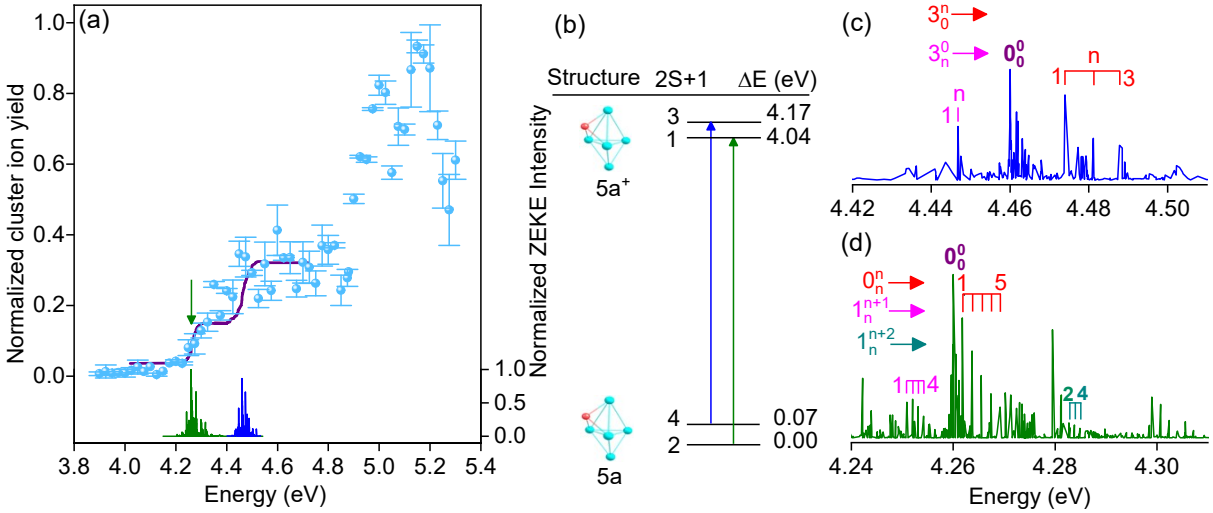

Fig. S4. (a) The simulated PI spectrum of Y_5O (violet solid line) is overlayed against the experimental spectrum (blue spheres). The calculated ZEKE spectra for the 2→1 and 4→3 ionization processes are shown below the PI spectrum in green and blue, respectively. The AIE is labelled with a solid green arrow. (b) DFT calculated the lowest-energy geometric structures and energy levels of the neutral and cation clusters of Y_5O. The simulated ZEKE spectra for Y_5O (c) 5a 4→3 and (d) 5a 2→1 ionization transition. Prominent vibronic transitions are assigned in the graph.

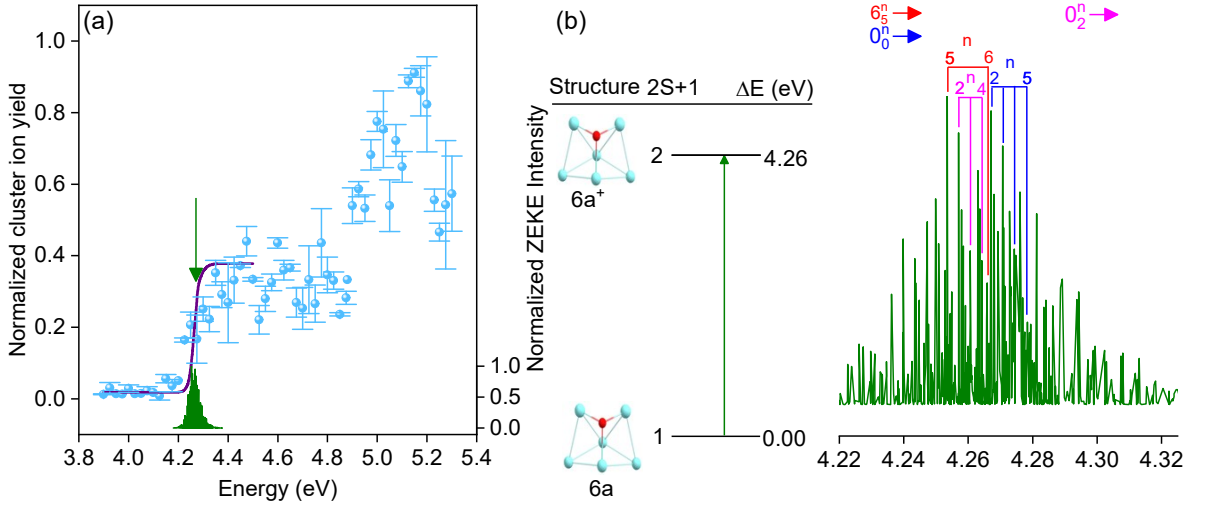

Fig. S5. (a) The simulated PI spectrum of Y_6O (violet solid line) is overlayed against the experimental spectrum (blue spheres). The calculated ZEKE spectrum for the 1→2 ionization process is shown below the PI spectrum in green. The AIE is labelled with a solid green arrow. (b) DFT calculated the lowest-energy geometric structures and energy levels of the neutral and cation clusters of Y_6O, and (c) The simulated ZEKE spectrum for the Y_6O 6a 1→2 ionization transition. Prominent vibronic transitions are assigned in the graph.

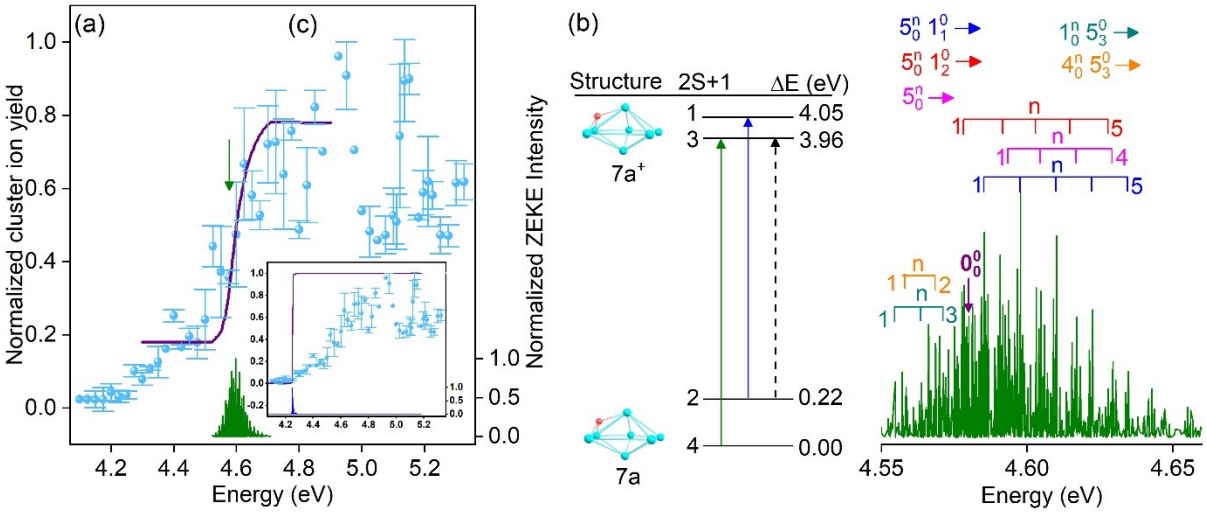

Fig. S6. (a) The simulated PI spectrum of Y_7O (violet solid line) is overlayed against the experimental spectrum (blue spheres). The calculated ZEKE spectrum for the 4→3 ionization process is shown below the PI spectrum in green. The AIE is labelled with a solid green arrow. In the inset, the simulated PI spectrum corresponding to the 2→1 transition is overlayed against the experimental spectrum, and corresponding ZEKE spectrum is shown below the PI spectrum in blue. The steeply sloped calculated PI spectrum does not correlate with the experimental PI spectrum. (b) DFT calculated the lowest-energy geometric structures and energy levels of the neutral and cation clusters of Y_7O, and (c) The simulated ZEKE spectrum for the Y_7O, 7a 4→3 ionization transition. Prominent vibronic transitions are assigned in the graph.

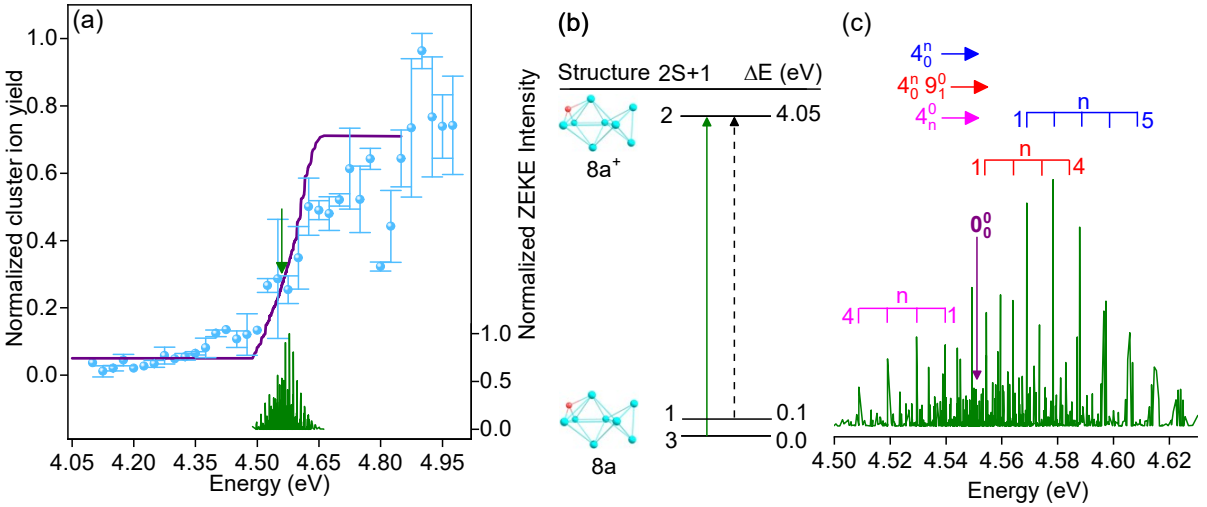

Fig. S7. (a) The simulated PI spectrum of Y_8O (violet solid line) is overlayed against the experimental spectrum (blue spheres). The calculated ZEKE spectrum for the 3→2 ionization process is shown below the PI spectrum in green. The AIE is labelled with a solid green arrow. (b) DFT calculated the lowest-energy geometric structures and energy levels of the neutral and cation clusters of Y_8O. The intensity of the 1→2 transition is stronger than the 3→2 transition. However, the 1→2 transition does not fit well with the experimental PI spectrum. (c) Simulated ZEKE spectrum of the 8a 3→2 ionization transition of Y_8O. Prominent vibronic transitions are assigned.

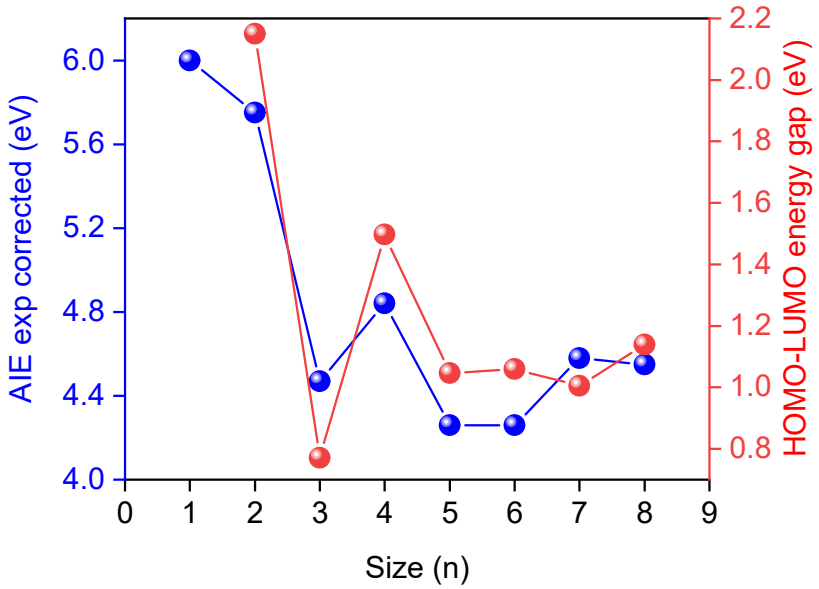

Fig. S8. Experimentally corrected AIEs along with the calculated HOMO– LUMO energy gaps are plotted as a function of cluster size, n.

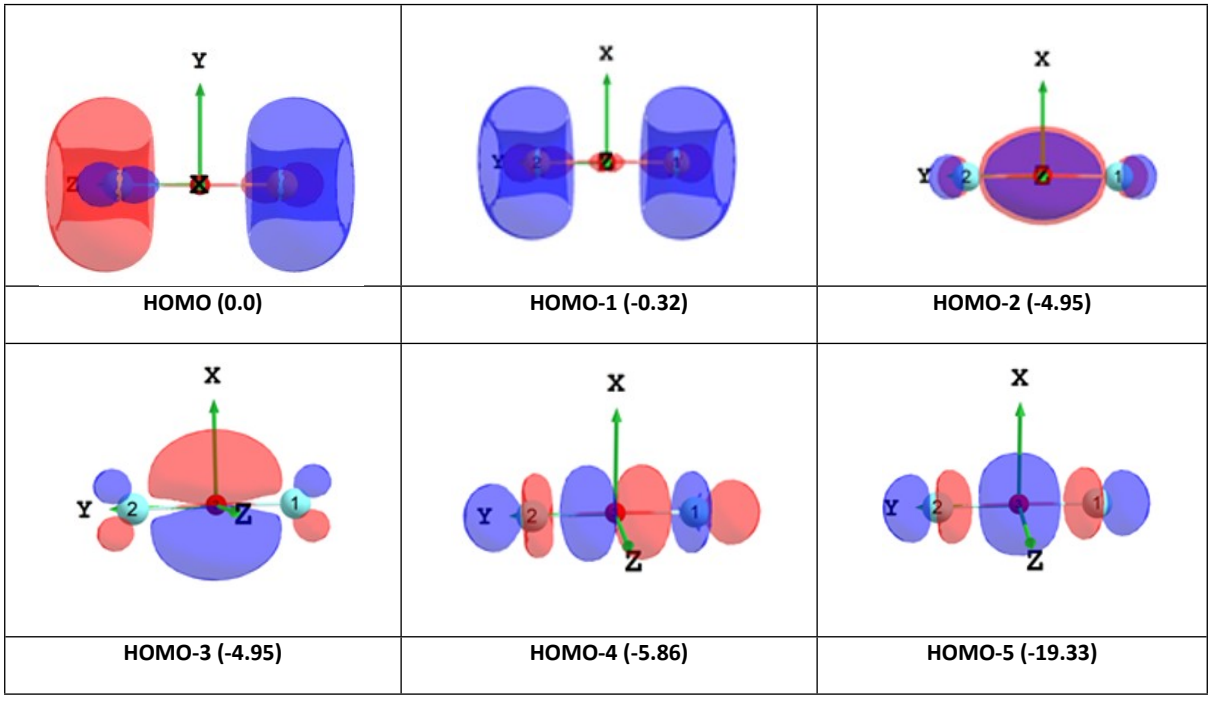

Fig. S9. Molecular orbitals (MOs) of Y_2O; energies in eV with respect to the HOMO as 0.0 are provided in parenthesis.

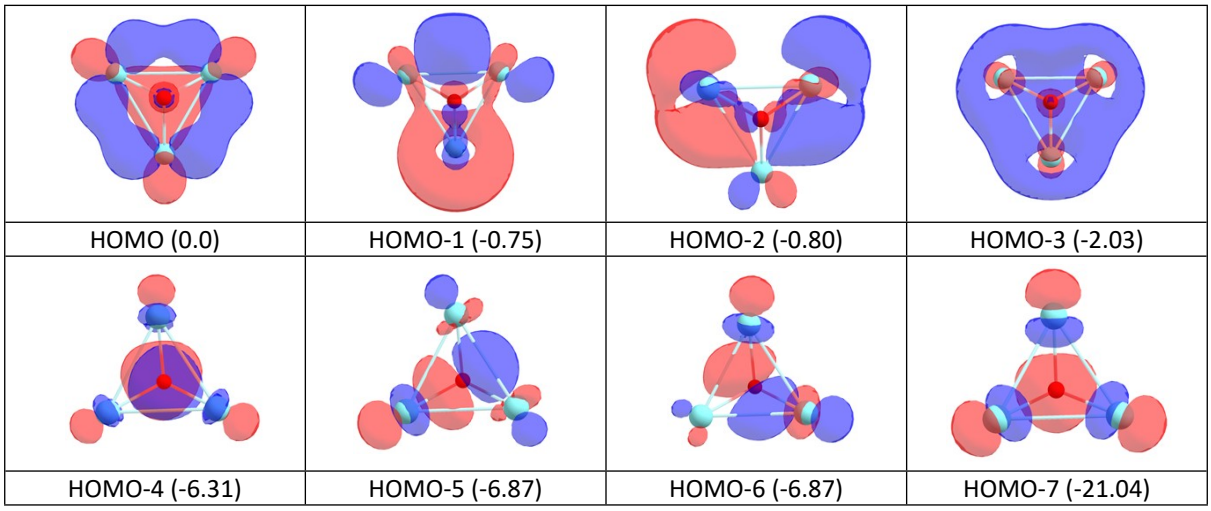

Fig. S10. Molecular orbitals (MOs) of Y_3O; energies in eV with respect to the HOMO as 0.0 are provided in parenthesis.

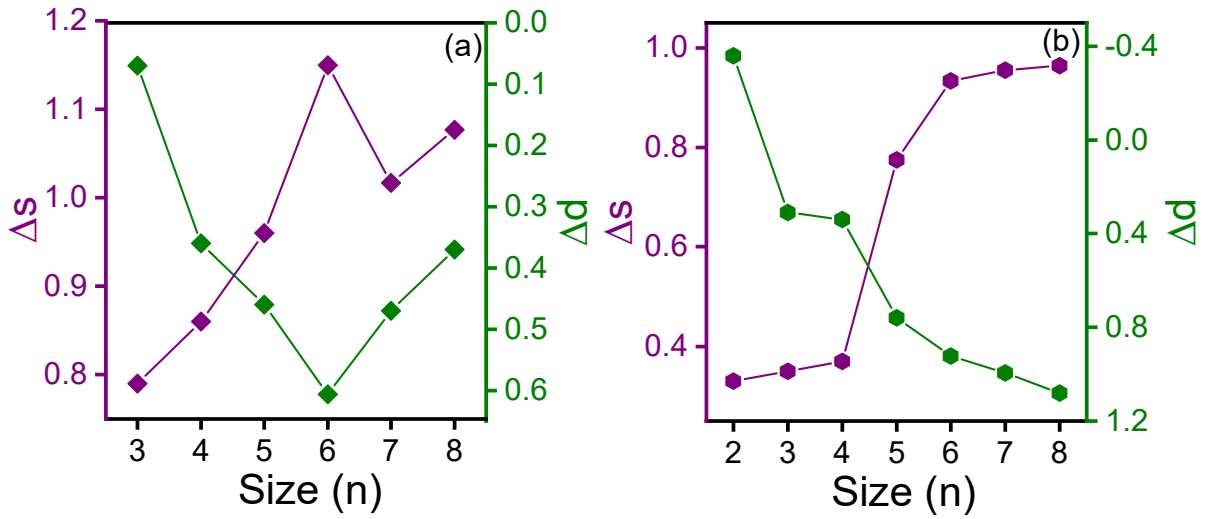

Fig. S11. (a) Average change in population of s and d atomic orbitals (Δs and Δd) of yttrium atoms which are bonded with oxygen atom in Y_nO clusters. (b) Δs and Δd for yttrium atoms which are not bonded with oxygen.

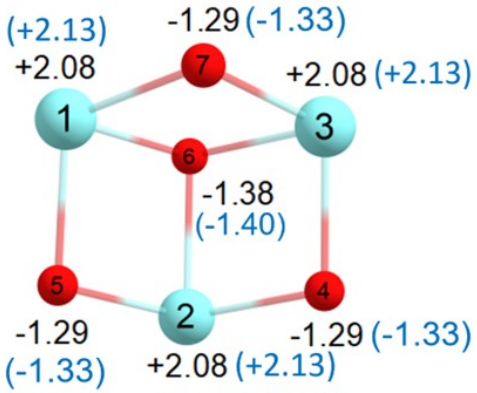

Fig. S12. Benchmarking of our NBO analysis. The charges reported by Misao et al. in *Phys. Chem. Chem. Phys.*, 2022, **24**, 11096–11103.The charges in parenthesis are our calculated values.

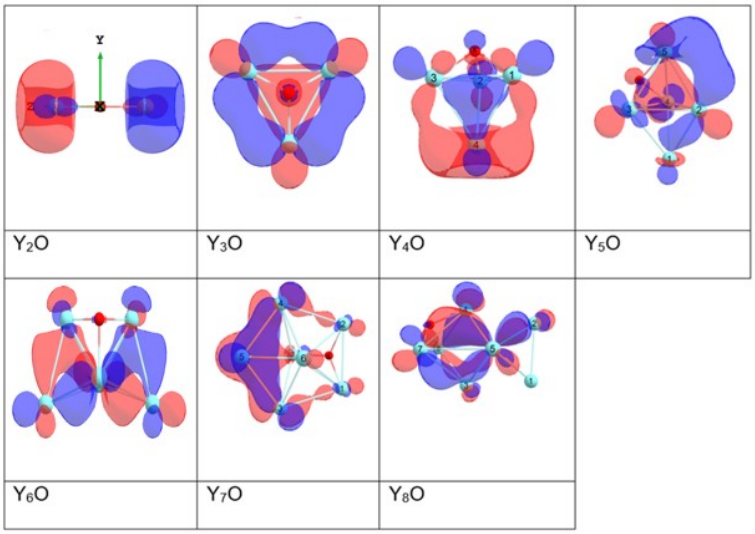

Fig. S13. HOMO orbitals of Y_nO (n = 2 – 8) clusters.

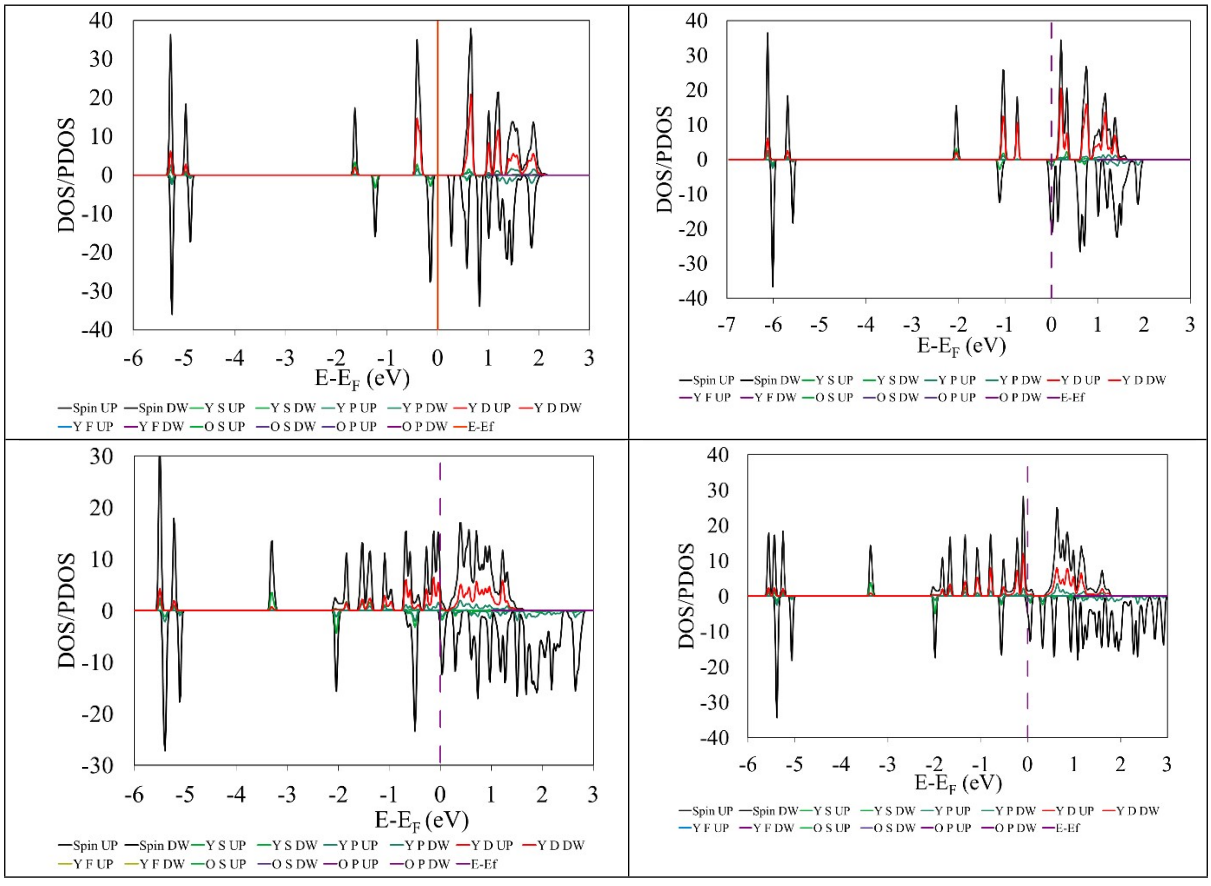

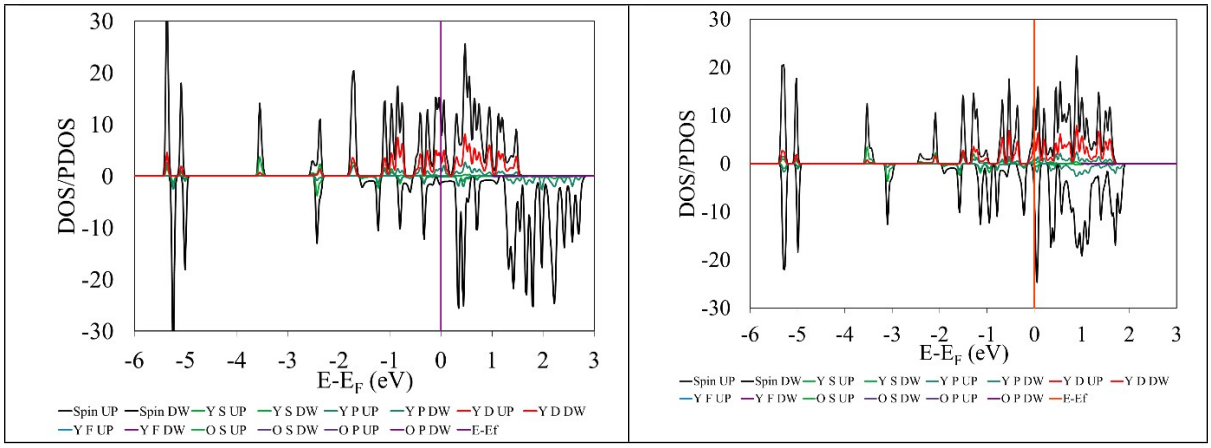

Fig. S14. The total density of states (DOS) and projected DOS of the ground state structures of Y_3O, Y_5O, and Y_6O clusters presented from respectively top to bottom on the left column and the corresponding cations are provided on the right. E_F is Fermi energy in eV.

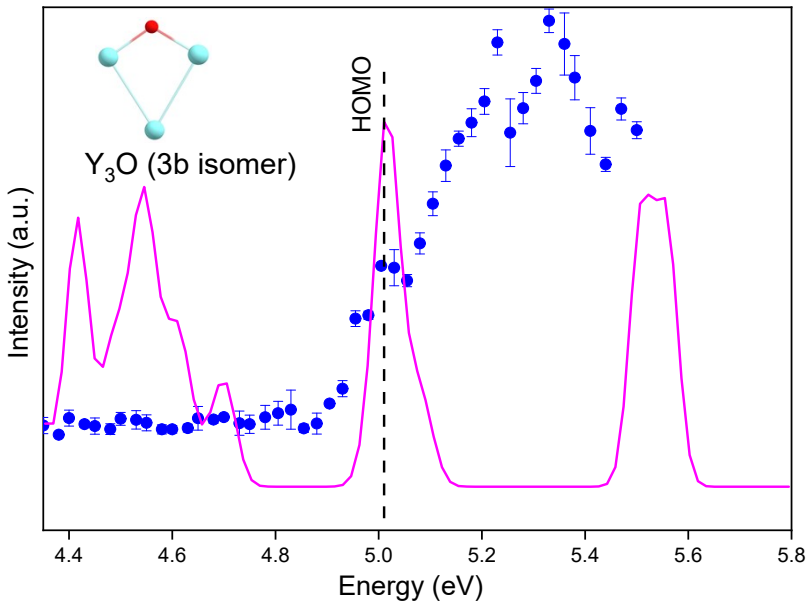

Fig. S15. Total density of states around the HOMO of the ground state isomers (magenta) of the neutral Y_3O (3b) cluster together with the experimental photoionization spectrum (blue spheres). The orbitals on the left of HOMO are unoccupied and higher in energy than HOMO and the orbitals on the right are occupied and lower in energy than HOMO. The first linear rise of ion intensity in the photoionization spectra is marked by a dotted line.